Ruddlesden Popper 2D Layered Perovskites as Li-ion Battery Electrodes

Supplementary information

Photoluminescence Characterisation of 2D Perovskite phases

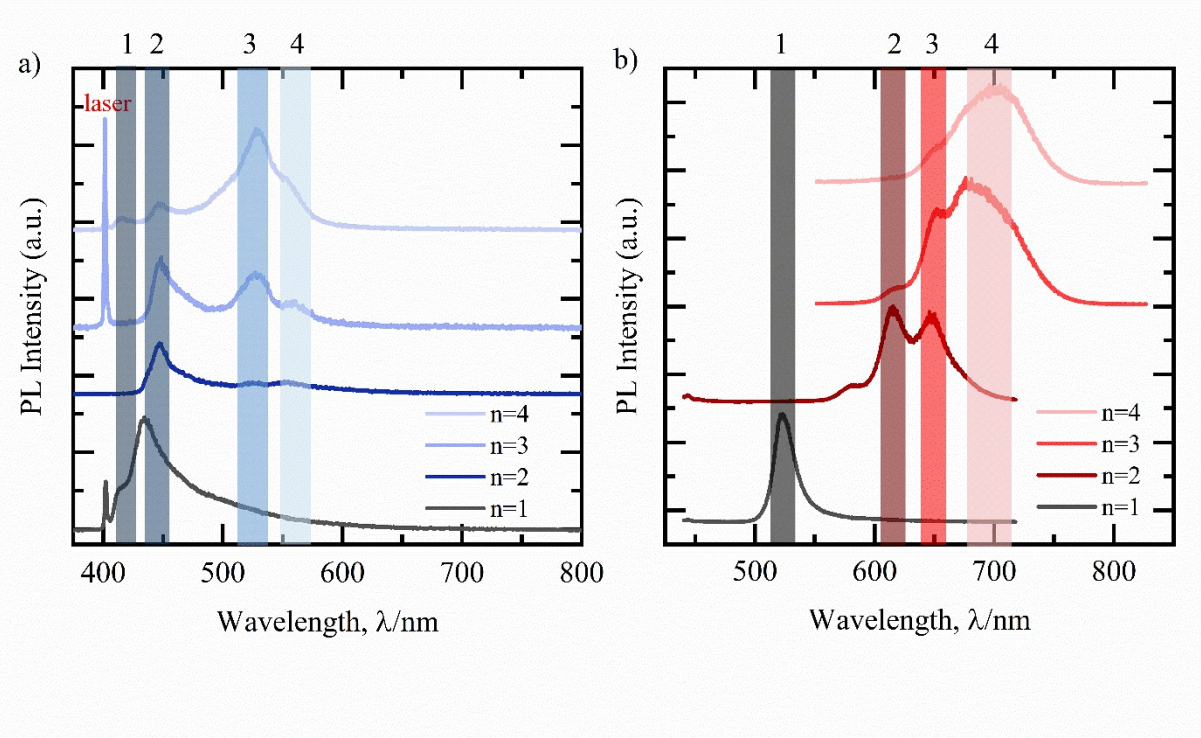

Figure S1: *PL spectra for the bromide-based* ***(a)*** *and iodide-based* ***(b)****, RP perovskite series from n=1 – n=4. Emission from multiple phases are detected for the n>1 species with an exaggerated emission intensity from higher order species due to charge channelling. The expected emission position from each pure-phase equivalent structure is highlighted and labelled above the figure. The position and shape of each spectrum confirms that the majority species present corresponds to the one intended by stoichiometry.*

Photoluminescence (PL) spectroscopy is used to probe the optoelectronic properties of the as-synthesised perovskite materials. The PL spectra shown for the iodide based layered perovskite series (**Figure S1 (a)**) and bromide-based series (**Figure S1 (b)**) conclude the formation of mixed phases upon deposition for the n>1 species. However, the relative intensities of the corresponding peaks confirm that each phase is unique and corresponds, predominantly, to the phase desired from the stoichiometric mixing of precursors during the perovskite synthesis. As expected, a distortion towards greater PL emission from the higher layered species is observed, due to charge channeling effects. The expected PL emissions from the corresponding layered species are labelled accordingly, with the expected trend of red-shifted emissions from the higher layering ordered species. This is in accordance with the results of the UV-Vis absorption measurements in **Figure 1** of the main text.

Synthesized material

a) b)

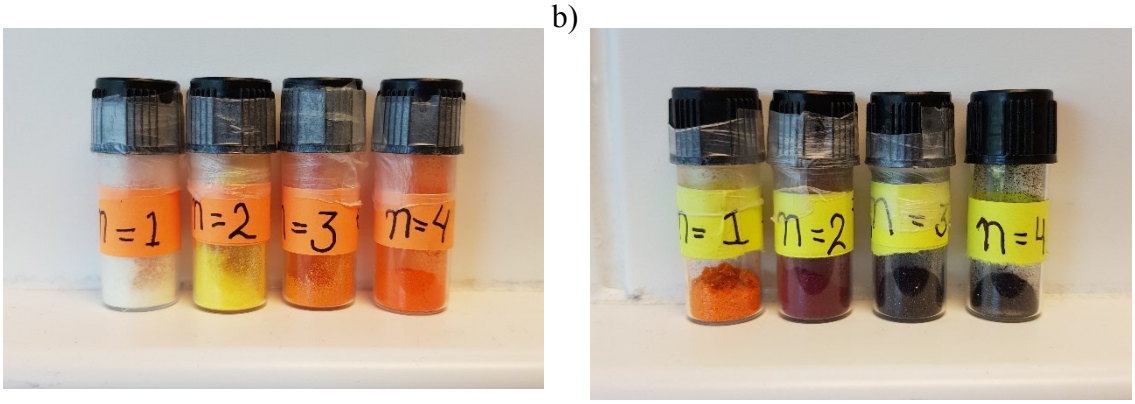

Figure S2: *Photographs of the perovskite materials as synthesised.* ***(a)*** *Bromide layered perovskite series from n=1 to n=4 (left to right).* ***(b)*** *Iodide layered perovskite series from n=1 to n=4 (left to right).*

$(BA)_2(MA)_{n-1}Pb_nI_{3n+1}$ Characterisation

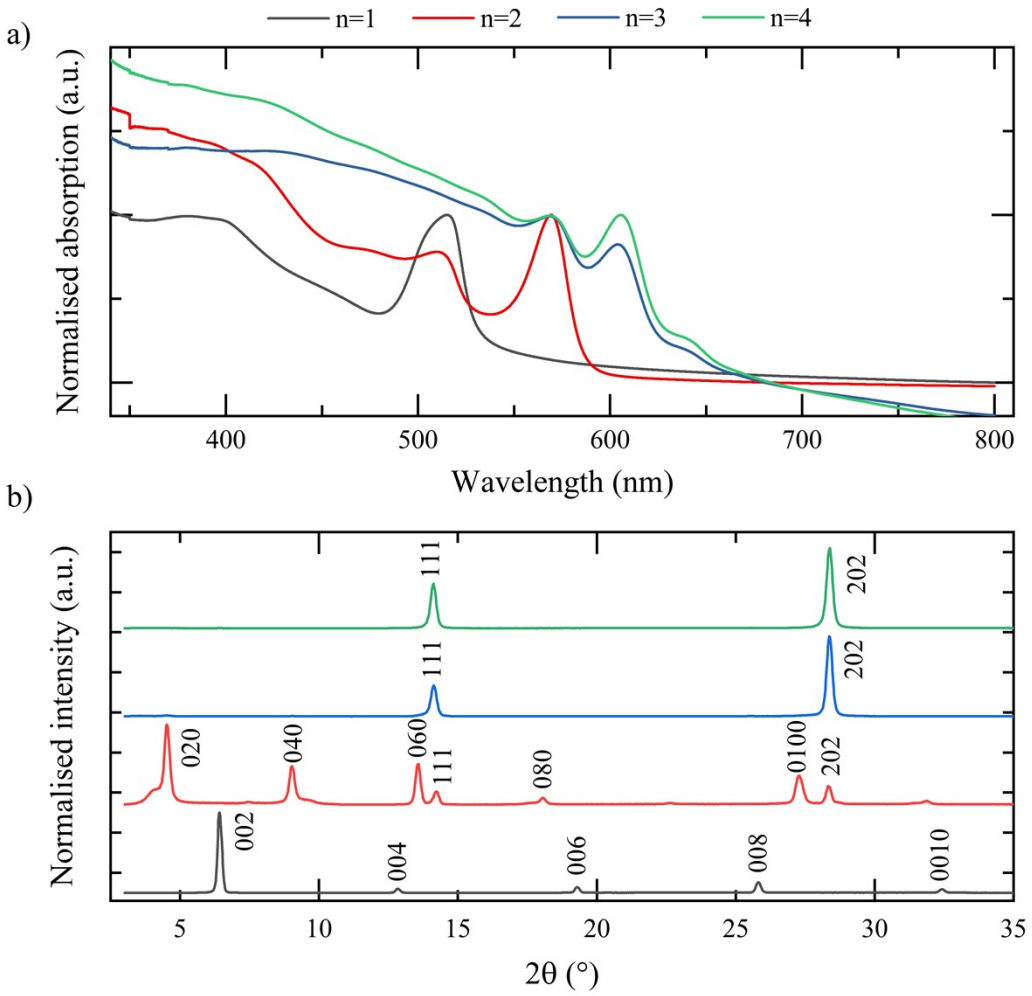

Figure S3: ***(a)*** *UV-vis absorption spectra of* $(BA)_2(MA)_{n-1}Pb_nI_{3n+1}$ *perovskite starting material as a function of n-number – the number of* $(MA)_{n-1}Pb_nI_{3n+1}$ *layers intercalated between the BA organic cations.* ***(b)*** *XRD spectra of the iodide-based starting perovskite materials as a function of n-number. The relevant diffraction peaks are labelled with their corresponding crystallographic orientations accordingly.*

Figure S3 shows the initial characterisation of the as-synthesised iodide-based layered perovskite materials $(BA)_2(MA)_{n-1}Pb_nI_{3n+1}$ – where n corresponds to the layering number. **Figure S3 (a)** demonstrates the changing optical absorption properties as a function of the layering number. It is demonstrated that an increase in the number of $(MA)_{n-1}Pb_nI_{3n+1}$ layers intercalated between the BA organic cation engenders a decrease in the absorption bandgap energy and a corresponding red-shift in the UV-vis absorption. The XRD spectra for the materials are shown in **Figure S3 (b)**.

Electrochemical characterisation of $(BA)_2(MA)_{n-1}Pb_nI_{3n+1}$ (Iodide-based RP series)

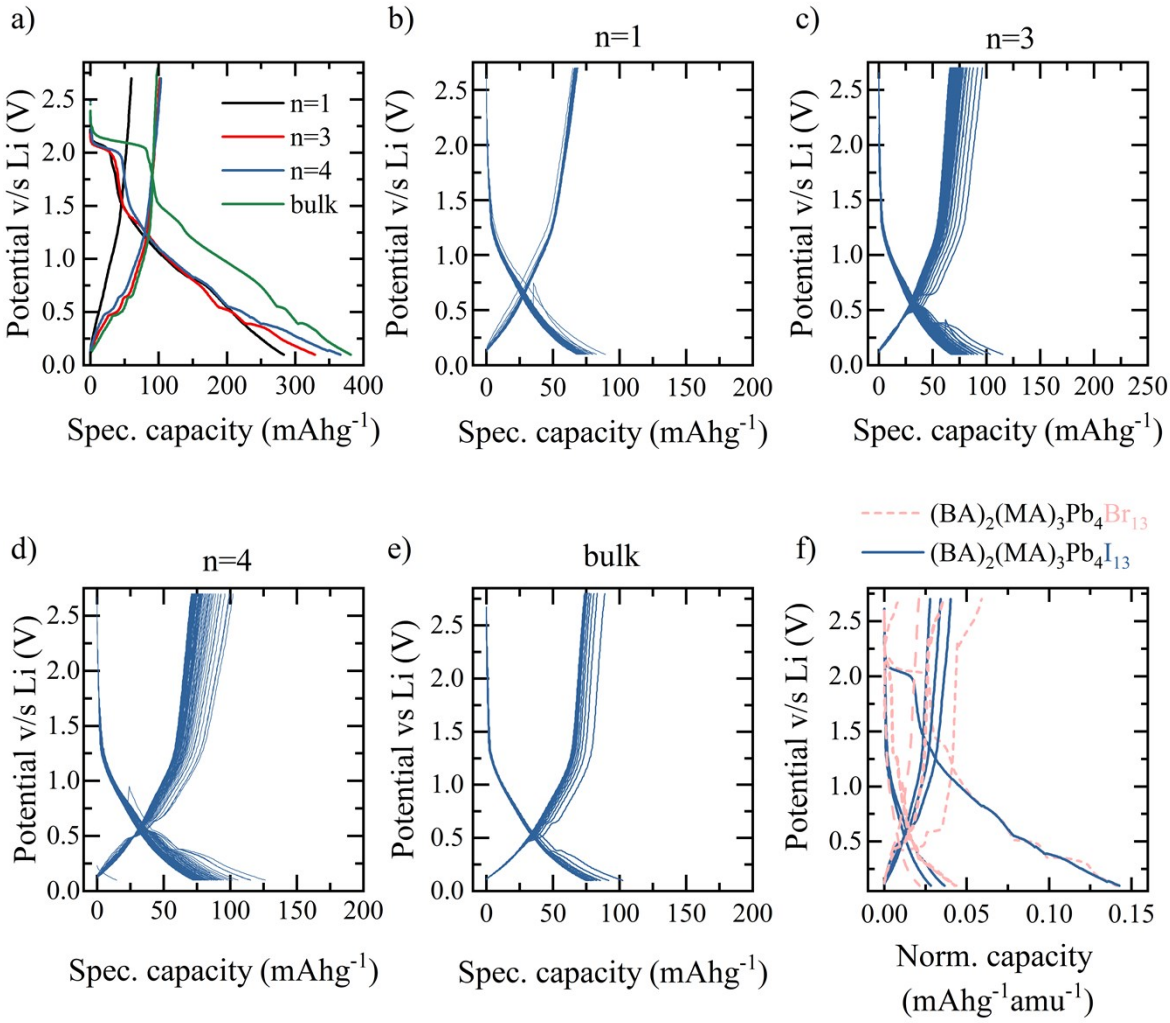

Figure S4: *Electrochemical characterisation of the iodide-based layered perovskite electrodes. All data taken at a current rate of 30 mAg^{-1}.* ***(a)*** *The first galvanostatic discharge and charge curves for the layering series from n=1 – n=4 and the bulk perovskite.* ***(b) – (e)*** *Subsequent (2nd onwards) galvanostatic charge-discharge cycles of the iodide-based layered perovskite series for n=1, 3, 4 and bulk.* ***(f)*** *The effect of changing the halide component of the perovskite battery electrode for n=4. The capacities are renormalized to remove the effect of the differing atomic weights of the halides and thus the gravimetric capacities. The first, 10th and 100th cycles are shown.*

Figure S4 (a) shows the first galvanostatic discharge and charge curves of the iodide-based layered perovskite electrodes. Similarly to the bromide based cells, an increase in the initial capacities is observed with the layering number.

Figure S4 (f) shows the effect of changing the halide composition of the layered perovskite electrode. The dashed (pink) line corresponds to the bromide based n=4 cell and the solid (blue) line the iodide based n=4 cell. The cell capacity is normalised in order to remove the effect of the differing atomic masses of bromide compared to iodide and thus the effect on the gravimetric capacities. It is shown that the different halides have very little effect on the overall electrochemical performance (judged by capacity and capacity retention) and electrochemical mechanism (judged by the positions and sizes of the various potential plateaus in the galvanostatic curve). This is despite the halide composition effecting other properties such as lattice spacing, electronegativity and crystallographic phase of the material.

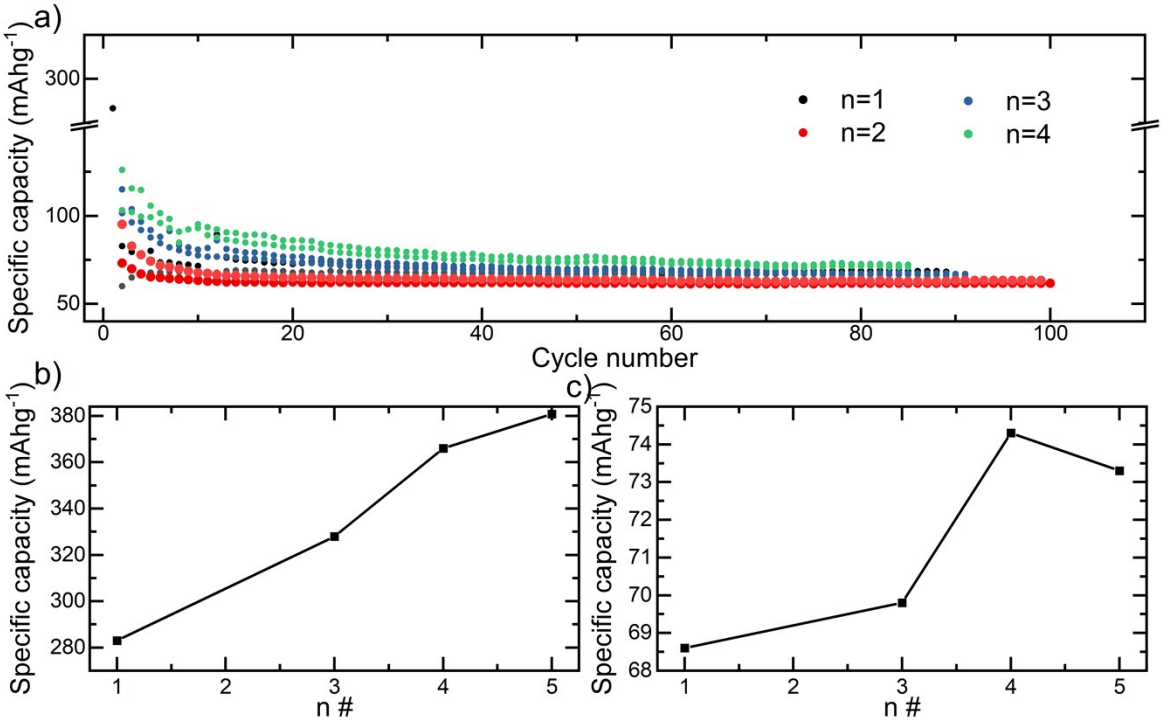

Figure S5: (a) *Gravimetric capacity of iodide perovskite series for the first 100 galvanostatic cycles.* ***(b)*** *Initial discharge capacity (capacity obtained during first discharge cycle) for iodide series.* ***(c)*** *Stabilised discharge capacity (taken after first 60 cycles and capacity appears stable) for the iodide series.*

Electrolyte analysis

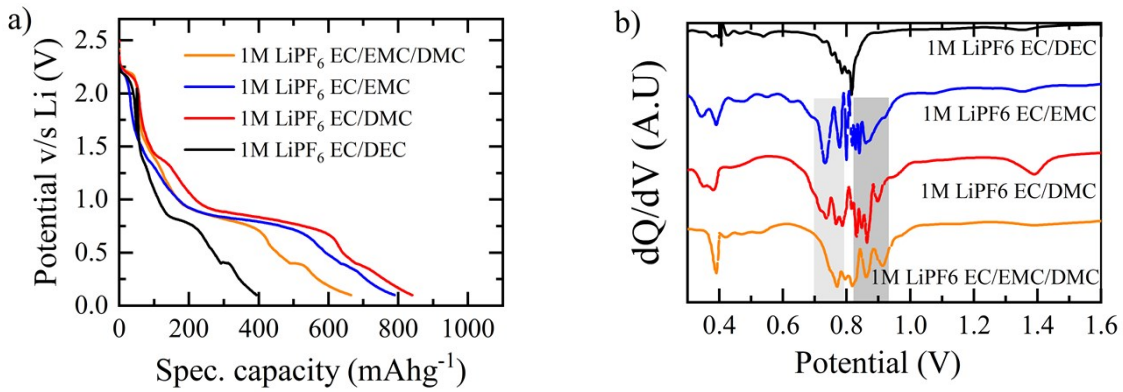

Figure S6: (a) *1st cycle discharge curves of* $BA_2MAPb_2Br_7$ *in 1M* $LiPF_6$ *electrolyte with different solvent composition. EC/DEC system shows smallest electrolyte decomposition and SEI formation plateau (~0.8V). The decomposition mostly contributes to specific capacity difference between EC/DEC and the rest systems.* ***(b)*** *the corresponding dQ/dV curves for all systems.*

Figure S6 (a) shows the discharge profile of $BA_2MAPb_2Br_7$ in 1M $LiPF_6$ $(EC/DEC\ 1{:}1)$, 1M $LiPF_6$ $(EC/EMC\ 1{:}1)$, 1M $LiPF_6$ (EC/DMC) and 1M $LiPF_6$ $(EC/EMC/DMC\ 2{:}1{:}1)$. The plateau at ~0.8 V is thought to correspond to electrolyte decomposition and SEI formation[1][2]. Such a process is irreversible. 0.8 V plateau width of EC/DEC is the shortest, suggesting SEI formation is less significant than the rest solvent systems. In dQ/dV curves in **Figure S6 (b)**, we notice a deeper left wing (light grey area) of EC/EMC and a deeper right wing (dark grey area) of EC/DMC. The shape of 0.7~0.95 V suggests a different decomposition process for DEC, EMC and DMC. EC/DEC is preferred to reduce capacity loss.

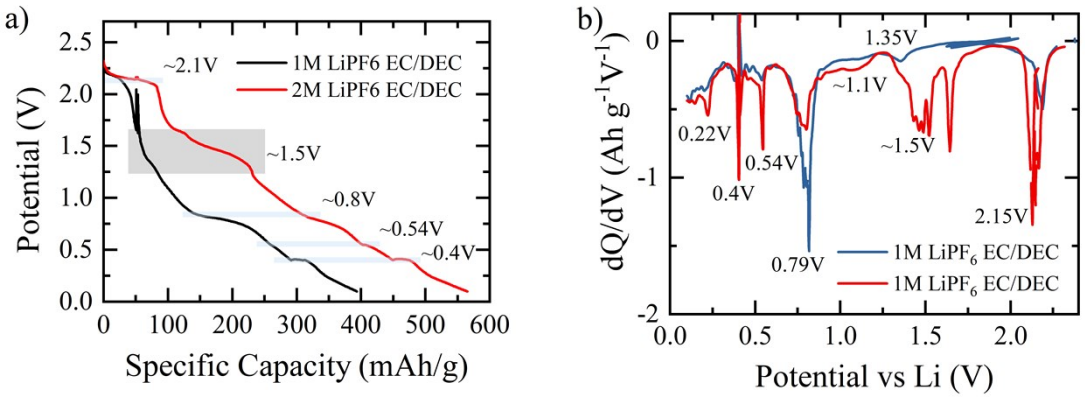

Figure S7: ***(a)*** *1st cycle discharge curves of* $BA_2MAPb_2Br_7$ *in 1M and 2M* $LiPF_6$ *(EC/DEC).* ***(b)*** *the corresponding dQ/dV curves.*

Figure S7 shows the 1st cycle discharge curves and dQ/dV curves for 1M and 2M $LiPF_6$ (EC/DEC). The reversible[3] Li-Pb alloying plateaus (0.22 V, 0.4 V, 0.54 V), lithium intercalation plateau (2.15 V) and perovskite decomposition plateau (~1.5 V) are larger on 2M than 1M. 1M shows larger electrolyte decomposition plateau (~0.8 V). Both suggests that high concentration lithium salt improves the intensity of reversible reactions.

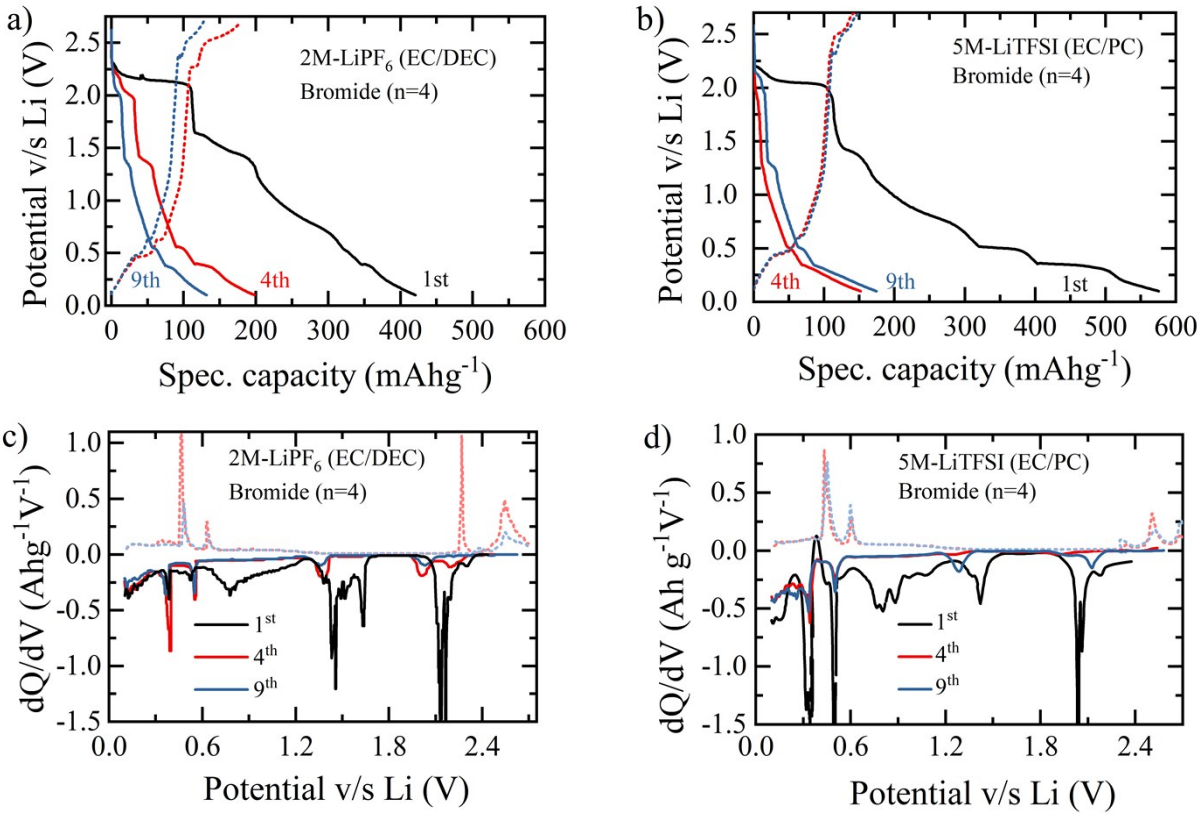

Figure S8: *charge and discharge profile of* $BA_2MA_3Pb_4Br_{13}$ *in* ***(a)*** *2M* $LiPF_6\ (EC/DEC)$ *and* ***(c)*** *5M* $LiTFSI\ (EC/PC)$. ***(b)*** *and* ***(d)*** *their corresponding dQ/dV curves. Dashed lines and solid lines correspond to charge and discharge curves respectively.*

Electrochemical performance of $BA_2MA_3Pb_4Br_{13}$ (layer number n=4) is compared between 2M $LiPF_6\ (EC/DEC)$ and 5M $LiTFSI\ (EC/PC)$. **Figure S8 (b)** and **Figure S8 (d)** show the Li-Pb alloying reactions are reversible, as shown by less decayed sharp peaks at ~0.4 V, ~0.5 V and ~ 0.45 V, ~0.60 V (charge). Irreversible peak region at 0.65-1.2 V also confirms the decomposition of electrolyte and formation of SEI layer. 2M $LiPF_6$ exhibits decayed 1.4 V peak (refers to perovskite decomposition[3]) on 4th and 9th discharge cycle. This suggests that perovskites are more soluble in dilute electrolytes. It is possible that 2M electrolyte dissolved the outer layer perovskite efficiently and consumed the inner layer material in early cycles,

while 5M electrolyte kept the inner layer material unreacted for multiple cycles and preserve higher capacity at the 9th cycle.

Electrochemical cell construction

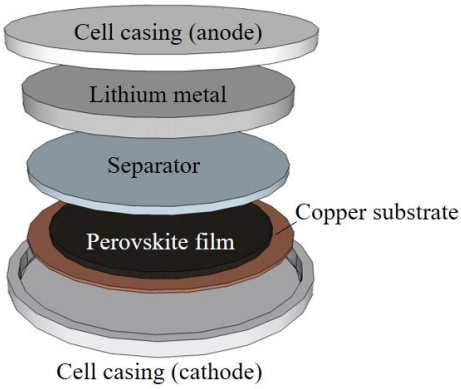

Figure S9: Schematic illustration of the electrochemical coin cell used for measuring the electrochemical properties of the perovskite electrodes.

Summary of lead-lithium alloy reactions

Reaction description	Potential, E^0 (V)
Pb + Li ↔ LiPb	0.601
LiPb + 2 Li ↔ Li_3Pb	0.449
Li_3Pb + 0.2 Li ↔ $Li_{3.2}Pb$	0.344
$Li_{3.2}Pb$ + 1.3Li ↔ $Li_{4.5}Pb$	0.292

Table S1: Summary of the multistage LixPb alloy reaction below 0.7 V in the perovskite electrode under voltaic cycling. Values from [Sean M.Wood, Codey H. Pham, Adam Heller, and C. Buddie Mullins. Communication - stages in the dynamic electrochemical lithiation of lead. Journal of The Electrochemical Society, 163(6):A1027–A1029, 2016].

Perovskite synthesis materials

Material	Description
N N-Dimethylformamide anhydrous (DMF)	99% purity, anhydrous, Sigma Aldrich
N-Butylammonium iodide (BAI)	Sigma-Aldrich
Methylammonium iodide (MAI)	>=99% purity, anhydrous, Sigma-Aldrich
N-Butylammonium Bromide (BABr)	98% purity, Sigma-Aldrich
Methylammonium bromide (MABr)	>=99% purity, anhydrous, Sigma-Aldrich
Lead iodide (PbI_2)	99.999% purity perovskite grade, Sigma-Aldrich
Lead bromide ($PbBr_2$)	98%, Scientific Laboratory Supplies

Table S2: List of precursors used for OHP synthesis.